International Symposium on Earthquake Engineering, JAEE, Vol.1, 2012

SEISMIC CAPACITY EVALUATION OF RC FRAME WITH URM WALL FOCUSED ON DIAGONAL STRUT MECHANISM

Kiwoong JIN[1], Ho CHOI[2], Noriyuki TAKAHASHI[2] and Yoshiaki NAKANO[3]

[1] Graduate Student, Graduate School of Eng., Department of Architecture, The University of Tokyo, Japan, kwjin@iis.u-tokyo.ac.jp
[2] Ph.D., Research Associate, IIS, The University of Tokyo, Japan, choiho@iis.u-tokyo.ac.jp, ntaka@iis.u-tokyo.ac.jp
[3] Ph.D., Professor, IIS, The University of Tokyo, Japan, iisnak@iis.u-tokyo.ac.jp

ABSTRACT: In this study, RC frames with URM (CB) wall for typical school buildings in Korea are experimentally investigated to evaluate their seismic capacity. One-bay, one-fourth scale specimens with CB walls having different boundary condition due to beam rigidity are tested under in-plain loading. In this paper, the diagonal strut mechanism of CB wall is discussed using principal compressive strains on CB wall. The lateral strength carried by CB wall and RC frame are also explained based on the compressive stress acting on CB wall and the curvature distribution along both columns during the test.

Key Words: RC building with URM wall, Seismic Capacity, Diagonal strut mechanism, FEMA306

INTRODUCTION

In some regions of Asia, Europe, and Latin America where earthquakes frequently occur, serious earthquake damage is commonly found resulting in catastrophic building collapse. Such damaged buildings often have unreinforced masonry (URM) walls, which are considered non-structural elements in the structural design stage, and building engineers have paid less attention to their effects on structural performance although URM walls may interact with boundary frames. The evaluation of seismic capacity of URM walls built in boundary frames is therefore urgently necessary to mitigate earthquake damage for those buildings.

For this purpose, RC frames with unreinforced concrete block (CB) wall for typical school buildings in Korea are experimentally investigated to evaluate their seismic capacity including failure mechanism and load bearing capacity. One-bay, 1/4-scale specimens with CB walls having different boundary condition due to beam rigidity are tested under cyclic and monotonic loadings. Among these specimens, the test results on inflled frame specimen with rigid beam under monotonic loading were discussed in the reference (Jin 2012). In this paper, the test results of two specimens with different boundary conditions due to beam rigidity under cyclic loadings are discussed.

OUTLINE OF EXPERIMENT

Prototype Building and Experiment Parameters

The test specimens are designed according to the standard design of Korean 4 story school buildings (referred to as "prototype building" shown in figure 1) in the 1980's (The Ministry of Construction and Transportation 2002). In this paper, two specimens which are infilled frame with rigid beam (IFRB) and infilled frame with flexible beam (IFFB) having an axial load level of their first story under cyclic loadings are discussed.

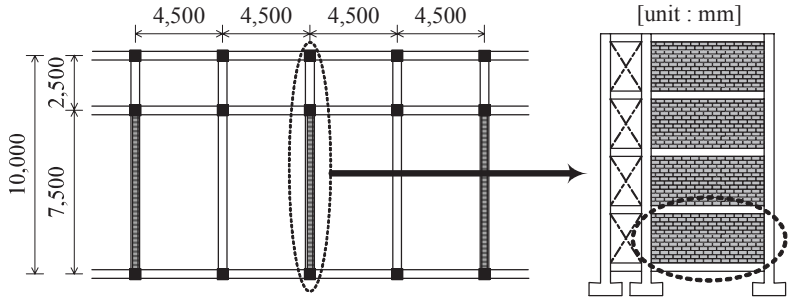

Fig. 1 Standard design of Korean 4 story school buildings in the 1980's

Design of Small-Scale Specimen

Figure 2 shows IFRB and IFFB specimens, which are the same as those tested under monotonic loadings. The design detail for each member is briefly described as follows.

Column and beam

The size of column section is 1/4 of that of prototype building. The axial stress in columns, the ratio of longitudinal reinforcement, and that of shear reinforcement are almost the same as the prototype building. As shown in figure 2(a), the upper beam of IFRB specimen is designed rigid enough to remain elastic even after columns and CB wall fail. On the other hand, specimen IFFB shown in figure 2(b) is designed to have steel columns above the upper beam to simulate the moment distribution of the prototype building. The upper beam with a rectangular section is designed to fail in flexure, where the shear-to-flexural strength ratio (Q_{SU} / Q_{MU}) and the flexural stiffness level are both similar to those of the prototype building.

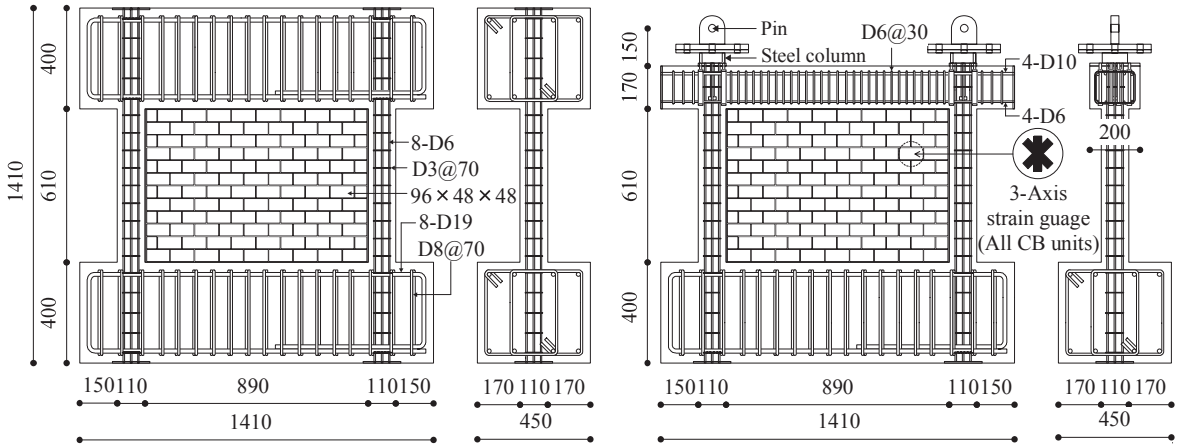

(a) BF specimen (b) IF specimen

Fig. 2 Details of specimens (unit : mm)

Concrete block units

The concrete block unit is 1/4 of that of the full-scale unit. It has three hollows inside and a half-sized hollow on each end as shown in figure 3 and photo 1. The cement-to-sand ratio is adjusted so that the strength and stiffness of three layered CB prism specimens should be close to those of the full-scale.

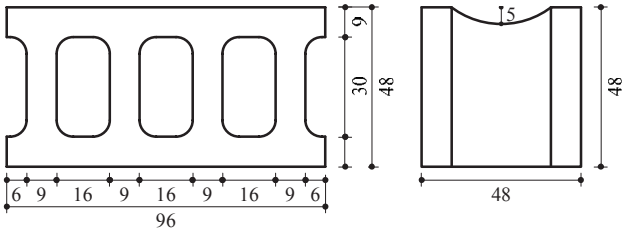

Fig. 3 Details of small scale CB unit (unit : mm)

Photo 1 Small scale CB unit

Material Characteristic

Tables 1 through 3 show the material test results, where the values represent the mean value of 3 samples in each test. Although the design strength of concrete specified in the standard design of Korean school buildings in the 1980's is 21*MPa*, the compressive strength of test pieces exceeds it as shown in Table 1. The yield strength of reinforcement shows higher values by 5 to 20% than the nominal strength. The compressive strength and Young's modulus from the 3 layered CB prism tests are around 90% and 60% of the full-scale CB prism, respectively. Although the Young's modulus of CB prism is not reproduced, it is found through previous investigations (FEMA306 1998) that the reduction of Young's modulus does not have much effect on the shear strength Vc of CB wall, and those 1/4-scale CB units are therefore applied to the test specimen.

Instrumentation and Loading Program

A three-axis strain gauge, which is attached on each CB unit (114 units) to estimate the equivalent strut width and the shear strength of CB wall, is the key point of the measurement plan (figure 2). Strains of longitudinal and shear reinforcement in columns of both specimens and in the upper beam of IFFB specimen are also measured.

Table 1 Mechanical properties of concrete (Mean value of 3 samples)

Compressive strength	Elastic modulus	Split tensile strength
29MPa	2.1×10^4MPa	2.4MPa

Table 2 Mechanical properties of reinforcement (Mean value of 3 samples)

Bar	Use / Member	Yield strength	Tensile strength	Young's modulus
D6 (SD345)	Main bar / Column	340MPa	516MPa	1.8×10^5MPa
D3 (SD390)	Hoop / Column	425MPa	495MPa	1.9×10^5MPa
D10 (SD295)	Top main bar / Flexural beam	365MPa	486MPa	1.9×10^5MPa
D6 (SD295)	Bottom main bar / Flexural beam	324MPa	397MPa	1.8×10^5MPa
D6 (SD785)	Stirrup / Flexural beam	862MPa	1,140MPa	1.9×10^5MPa

Table 3 Mechanical properties of concrete block (Mean value of 3 samples)

Concrete Block Prism*	
Compressive strength	Young's modulus
6.5 (7.3)MPa	1.1 (2.0)$\times10^4$MPa

* 3 layered specimen, ( ) : Material test results of full-scale CB unit

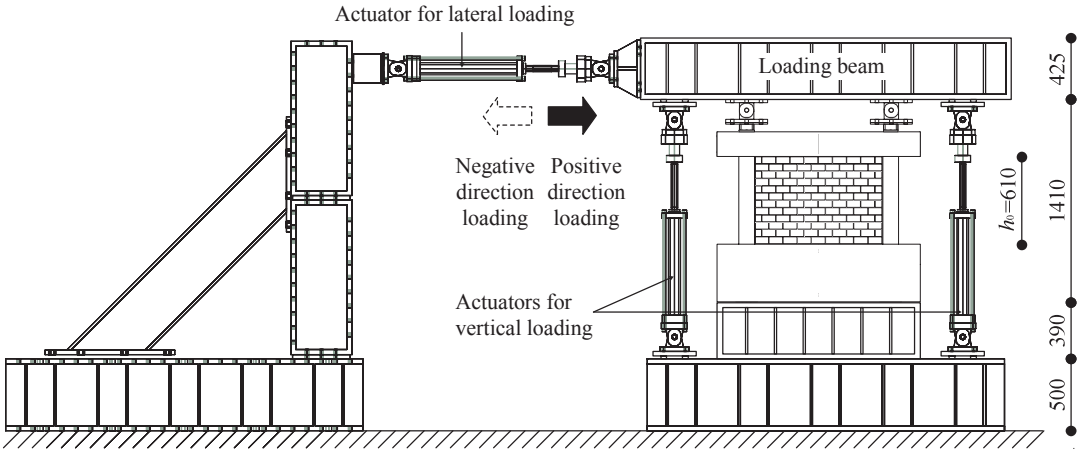

Fig. 4 Test setup of IFFB specimen (Unit : mm)

The loading system of IFFB specimen is shown in figure 4. Cyclic lateral loads are applied to each specimen through the loading beam tightly fastened to the specimen. Peak drift angles of 0.1, 0.2, 0.4, 0.67, 1.0, 1.5, 2.0, and 3.0% are planned, and 2.5 cycles for each peak drift are imposed to eliminate one-sided progressive failure (unsymmetric failure pattern in positive or negative loadings). Herein, a peak drift angle (R) is defined as" lateral deformation (δ) / column height (h_0=610mm)". It should also be noted that 0.4% loading is imposed after 1.0% to investigate the effect of small amplitude loading (i.e., aftershocks) after large deformation. A constant axial load of 96kN (4.0MPa) is applied to each specimen.

TEST RESULTS

IFRB Specimen

As shown in figure 5(a) and figure 6(a), cracks in joint mortar between CB units and flexural cracks in tensile column occur at the drift angle of 0.1%. During 0.2% loading, a flexural crack in compression column and a clear shear crack at the top of tensile column are observed. The maximum strength of 61kN is recorded at the drift angle of 0.4% shortly after the longitudinal reinforcement in tensile column yields. A shear crack at the bottom of compression column is observed during 0.67% loading, and the longitudinal reinforcement in compression column yields at the drift angle of 0.8%. During 1.5%

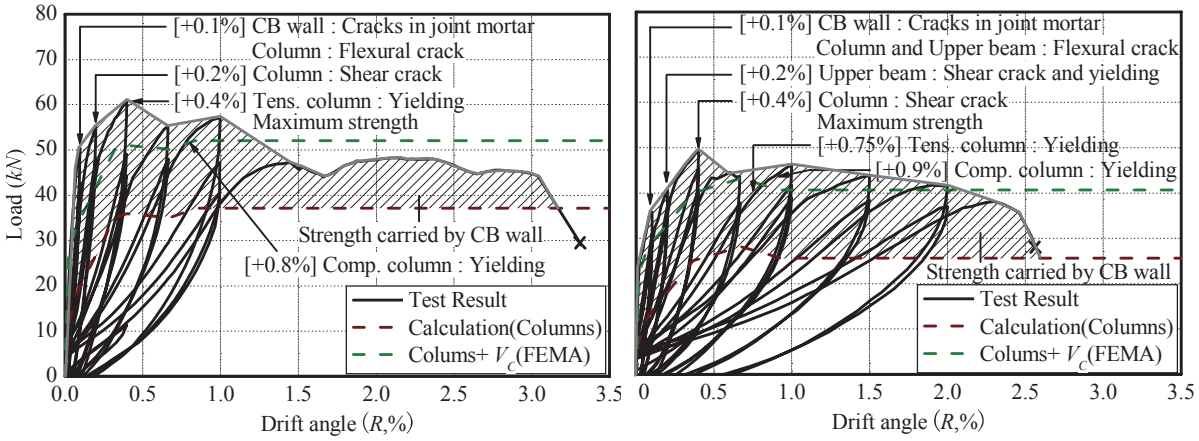

(a) IFRB specimen (b) IFFB specimen

Fig. 5 Lateral strength and drift angle relation

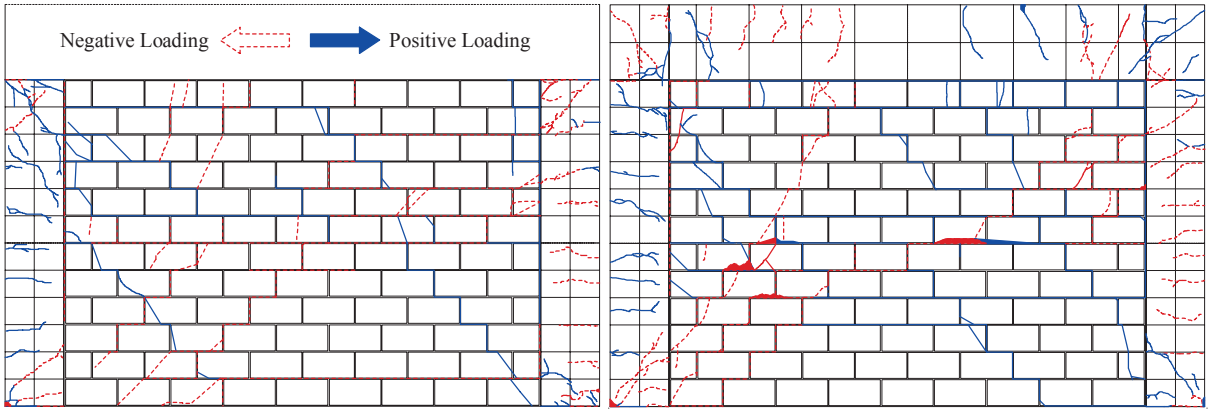

(a) IFRB specimen (b) IFFB specimen

Fig. 6 Crack patterns in both specimens

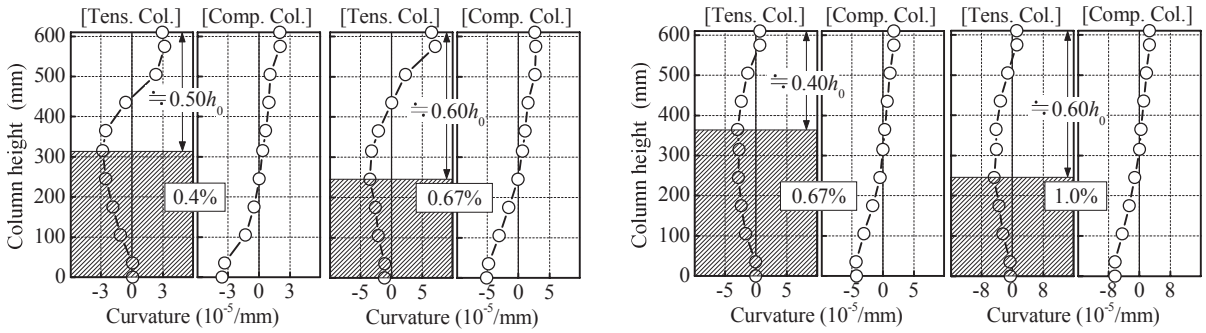

(a) IFRB specimen (b) IFFB specimen

Fig. 7 Curvature distribution of columns in both specimens

loading, shear cracks at the top of tensile column largely open at the drift angle of 1.45% resulting in sudden deterioration of lateral strength, but no remarkable strength degradation is observed until 3.0% loading. Finally, a sudden shear failure occurs resulting from rapid opening of shear cracks at the top of tensile column and the bottom of compression column at this drift angle.

In order to calculate the lateral strength of both columns, which is shown in figure 5(a), the initial stiffness (K_c), secant stiffness ($\alpha_y \cdot K_c$), and cracking moment (M_c) of column herein are calculated according to the reference (AIJ 2010). The ultimate bending moment M_u of columns is also calculated based on the plane-section assumption setting the ultimate strain ε_{cu} at the compression fiber of concrete equal to 0.003 with an equivalent rectangular stress block coefficient 0.85 (AIJ 1988). The observed curvature distribution in both columns at the drift angle of 0.4% and 0.67% are shown in figure 7(a). As shown in the figure, the tensile column behaves as a short column due to CB wall, and the effective height of tensile column is therefore assumed as $0.5h_0$ and $0.6h_0$, respectively, before and after the drift angle of 0.67%, while that of compression column is assumed as h_0. The shear strength V_C of CB wall is then calculated according to equations (1) and (2) (FEMA306 1998), and the sum of shear force of RC columns and CB wall is shown in figure 5(a), which does not show good agreement with the overall lateral strength.

$$V_C = a_{eq} \cdot t \cdot f_m \cdot \cos\theta_m \tag{1}$$

$$a_{eq} = 0.175 \cdot \left(\frac{4 \cdot E_c \cdot I_c \cdot h_m}{E_m \cdot t \cdot \sin 2\theta_m \cdot h^4} \right)^{0.1} \cdot l_d \tag{2}$$

in which a_{eq} : equivalent strut width, t : thickness of CB wall, f_m : 50% of prism strength, θ_m : angle of CB wall height to length, E_c : Young's modulus of concrete, I_c : moment of inertia of column, h_m : height of CB wall, E_m : Young's modulus of CB prism, h : column height, and l_d : diagonal length of CB wall.

IFFB Specimen

As shown in Fig. 5(b) and Fig. 6(b), vertical and horizontal cracks in joint mortar between CB units, as well as flexural cracks in tensile column and the upper beam, develop at the drift angle of 0.1%. A shear crack in the upper beam is observed at the drift angle of 0.2%, and longitudinal reinforcement in the beam also yields at this drift angle. During 0.4% loading, a shear crack in tensile column occurs and the maximum strength of 49.5kN is recorded. The yielding drift angles of the longitudinal reinforcement in tensile and compression columns are about 0.75% and 0.9%, respectively. No remarkable strength deterioration is found until the drift angle of 2.3%, but shear cracks at the top of tensile column and the bottom of compression column rapidly open at this drift angle, resulting in a shear failure with sudden deterioration of the lateral load carrying capacity.

The total lateral strength calculated in both columns is shown in figure 5(b), and the curvature of both columns at the drift angles of 0.67% and 1.0% are shown in figure 7(b). As shown in figure 7(b), the tensile column in this specimen behaves as a cantilever column. Based on this result, the effective height of tensile column is assumed as $0.4h_0$ and $0.6h_0$, respectively, before and after the 1.0% drift angle, while that of compression column is assumed as h_0. The shear strength V_C of CB wall previously calculated is then added to the shear force of RC columns (figure 5(b)), and their sum does not agree well with the overall lateral strength as can be found in IFRB specimen.

EQIVALENT DIAGONAL STRUT AND SHEAR STRENGTH OF CB WALL

In this section, the equivalent diagonal strut mechanism of CB wall including its main angle, average compressive strain, and equivalent width is discussed based on the strain values of 3-axis strain gauges on CB units measured during the test as is done in the reference (Jin 2012). The shear load carried by the CB wall is then evaluated using the compressive stress acting in the equivalent diagonal strut width calculated from the element experiments of CB prisms which will be discussed later. In this paper, equivalent diagonal strut mechanism at the maximum strength drift angle (0.4%) in both specimens is representatively described in detail

Equivalent Diagonal Strut of CB Wall

The main angle, average compressive strain, equivalent width, and central axis of equivalent diagonal strut of CB wall is evaluated as described below.

Principal compressive strain and its angle of each CB unit

The principal compressive strain and its angle of each CB unit are first calculated according to the conventional equations (3) through (5) from the strain values of 3-axis strain gauges on CB Wall. Figure 8 shows the principal compressive stain and its angle of each CB unit at the drift angle of 0.4% in both specimens. As can be found in the figure, most principal compressive strain of CB units diagonally distributes with respect to the horizontal line.

$$\varepsilon_{1,2} = \frac{\varepsilon_x + \varepsilon_y}{2} \pm \sqrt{\left(\frac{\varepsilon_x - \varepsilon_y}{2}\right)^2 + \left(\frac{\gamma_{xy}}{2}\right)^2} \tag{3}$$

$$\gamma_{xy} = 2\varepsilon_{xy} - \left(\varepsilon_x + \varepsilon_y\right) \tag{4}$$

$$\tan 2\theta_2 = \frac{\gamma_{xy}}{\varepsilon_x - \varepsilon_y} \tag{5}$$

in which ε_1 : principal tensile strain, ε_2 : principal compressive strain, ε_x and ε_y : diagonal direction strains on CB unit, ε_{xy} : the vertical direction strain of CB unit shown in figure 5, γ_{xy} : shear strain, and θ_2 : principal compressive strain angle with respect to the horizontal direction.

Main diagonal strut angle of CB wall

The main diagonal strut angle representing the diagonal strut of CB wall is then estimated from the

principal compressive strain and its angle of each CB unit. In this study, the average of the principal compressive angle weighted with its strain is employed to calculate the main diagonal strut angle θ as shown in equation (6). As shown in the equation, strains ε_{2j} with angles between 0° through 90° are only employed. From the calculation results, the main diagonal strut angle are about 42° and 47° in IFRB and IFFB specimens, respectively.

$$\theta = \left(\sum_{j=1}^{m} \varepsilon_{2j} \times \theta_{2j} \right) / \sum_{j=1}^{m} \varepsilon_{2j} \quad (0^0 \le \theta_{2j} \le 90^0) \tag{6}$$

in which ε_{2j} and θ_{2j} : principal compressive strain and angle of CB unit, and m : number of CB units with θ_{2j} between 0° and 90°.

Principal compressive strain distribution along the diagonal strut

As shown in figure 9, the CB wall is divided to 15 sections at an equal interval in the diagonal direction, and the mean value of principal compressive strains ε_i of CB units included in section i (i=1 to 15) is calculated. The principal compressive strains with angles between 0° through 90° are only considered herein as is done earlier. As can be seen in the figure, the mean value ε_i shows nearly a symmetric distribution with concave shape at the drift angle of 0.4% in both specimens. The average value of principal compression strain of 15 sections (average principal compression strain ε_m) shown in figure 9 is about 240μ and 220μ in IFRB and IFFB specimens, respectively.

Effective strut width and equivalent diagonal strut width

The effective strut width $W_{e,i}$ in each section at 0.4% drift loading is shown in figure 10, which is defined as the outmost distance of CB units having principal angle in the range of 0° through 90°. In both specimens, the effective strut width shows nearly a symmetric distribution with convex shape as

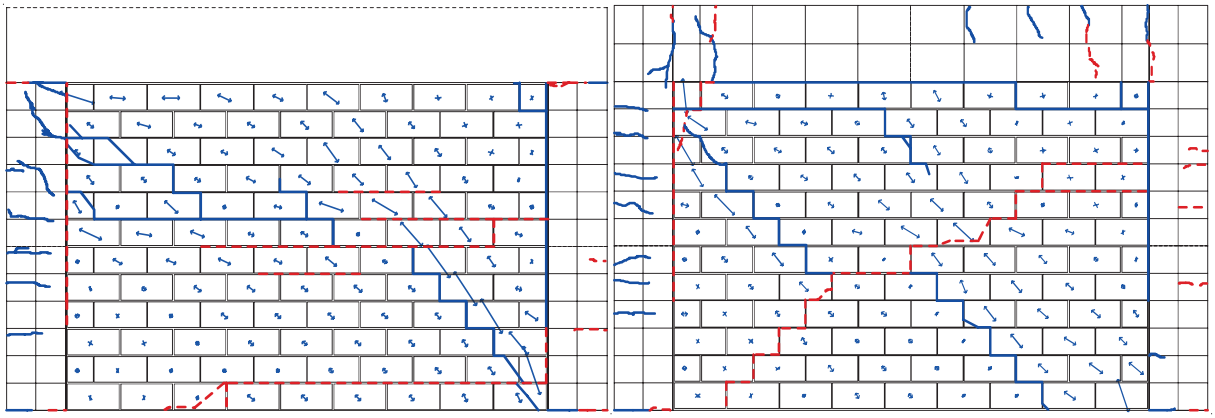

(a) IFRB specimen (b) IFFB specimen

Fig. 8 Principal compressive strain (0.4%)

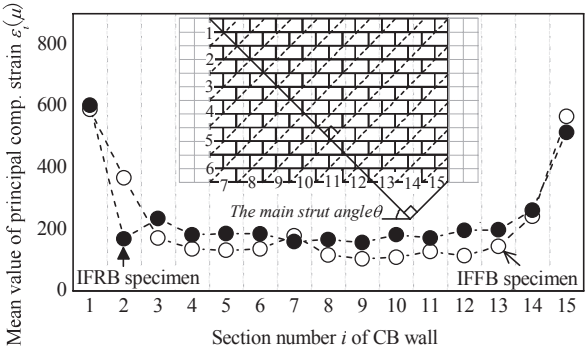

Fig. 9 Mean value of comp. strain in each section (0.4%)

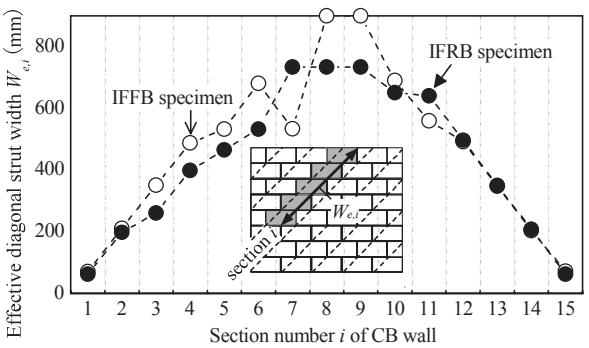

Fig. 10 Effective strut width in each section (0.4%)

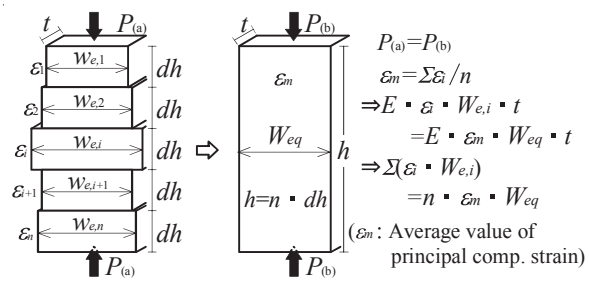

(a)Original strut (b)Equivalent strut

Fig. 11 Equivalent diagonal strut width

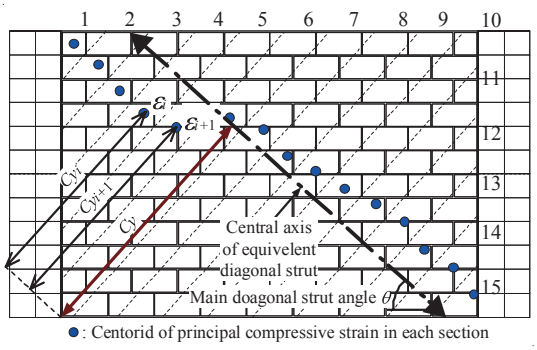

Fig. 13 Central axis of diagonal strut

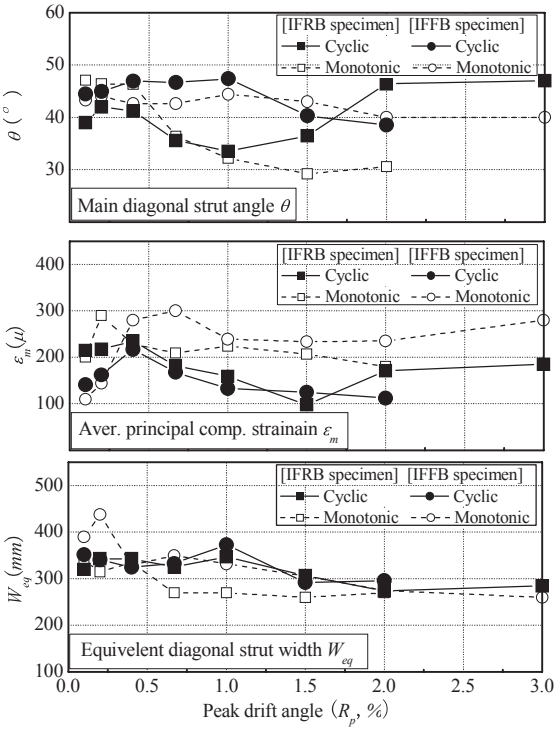

Fig. 12 Distribution of θ, ε_m, and W_{eq}

shown in the figure. The equivalent diagonal strut width W_{eq} is then evaluated according to equation (7), which assumes that the same compression force P is applied to the equivalent strut section as shown in figure 11. They are about 340mm and 325mm in IFRB and IFFB specimens, respectively.

$$W_{eq} = \left(\sum_{i=1}^{n} (\varepsilon_i \times W_{e,i}) \right) / \sum_{i=1}^{n} \varepsilon_i \tag{7}$$

in which ε_i and $W_{e,i}$: mean value of principal compressive strain and effective strut width in section i, and n : 15.

The distribution of main diagonal strut angle θ, average principal compression strain ε_m, and equivalent diagonal strut width W_{eq} under cyclic loadings are compared to those under monotonic loadings along with the peak drift angle in both specimens in figure 12. As shown in the figure, the main diagonal strut angle θ of IFFB specimen (shown in "●") under cyclic loadings has higher values than that of IFRB specimen (shown in "■") until the drift angle of 1.5%, since larger vertical compression force acts on CB wall of IFFB specimen due to its beam deformation. This tendency is similar in those specimens under monotonic loading. The average principal compression strains ε_m of IFRB and IFFB specimens are lower than those under monotonic loadings because of different loading method. For equivalent diagonal strut width W_{eq}, only IFRB specimen under monotonic loading is found slightly smaller than other specimens from the test results.

Central axis of diagonal strut

The distance of centroid Cy_i of principal compressive strain of CB units in each section (i) is first calculated according to equation (8) and they are plotted by ● in figure 13. The central axis of the diagonal strut C_y is then estimated according to equation (9) and shown in the figure. Figure 14 shows equivalent diagonal strut evaluated at the drift angle of 1.0%, where their main strut angles are totally different in both specimens.

$$Cy_i = \left(\sum_{i=1}^{m} \varepsilon_{2i} \times y_{2i} \right) / \sum_{i=1}^{m} \varepsilon_{2i} \tag{8}$$

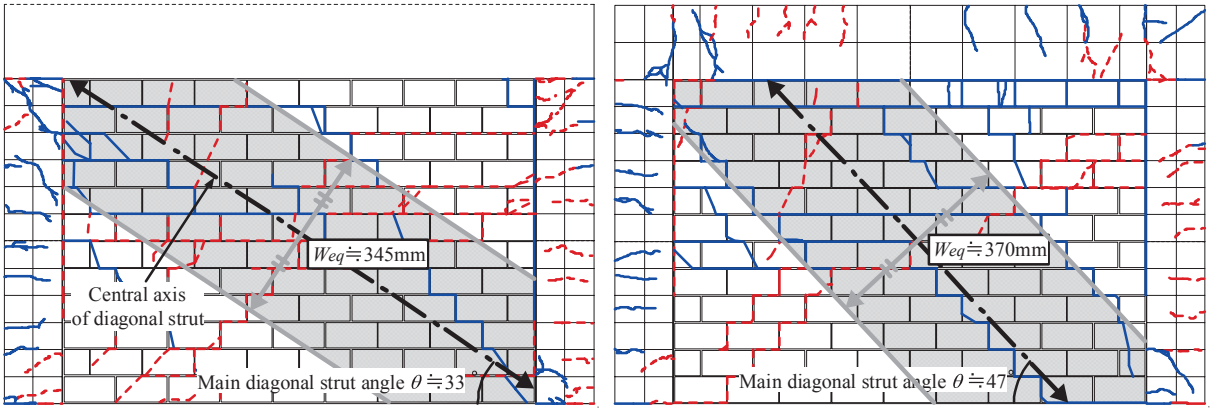

(a) IFRB specimen (b) IFFB specimen

Fig. 14 Equivalent diagonal strut in both specimens (1.0%)

$$Cy = \left(\sum_{i=1}^{n} \varepsilon_i \times Cy_i \right) / \sum_{i=1}^{n} \varepsilon_i \tag{9}$$

in which ε_{2i} : principal compressive strains of CB units in section i, y_{2i} : distance to each center of principal compressive strain in section i perpendicular to the main strut angle, ε_i : mean value of principal compressive strain of CB units in section i, m : number of CB units with θ_{2j} between 0° and 90° in section i, and n : 15.

Estimation of Shear Strength of CB Wall

In this section, the shear strength V_{cs} of CB wall is evaluated according to equation (10). In the equation, σ_m is the principal compressive stress corresponding to the average principal compressive strain ε_m of equivalent diagonal strut. In this study, the stress (σ_m)-strain (ε_m) relationship is obtained from the element tests using CB prisms as shown in figure 15, where the parameter is main diagonal strut angles (θ= 45°, 37.5°, 30°). The σ_m -ε_m relationships until the maximum ε_m calculated from the CB walls in both specimens during the tests are shown in figure 16, and they have similar results to one another until the maximum ε_m. The σ_m -ε_m relationship, which is most close to main diagonal strut angle from equation (6), is then employed to calculate the shear strength of CB wall.

$$V_{cs} = W_{eq} \cdot t \cdot \sigma_m \cdot \cos\theta \tag{10}$$

in which W_{eq} : equivalent diagonal strut width, t : wall thickness, σ_m : compressive stress corresponding to the average compressive strain ε_m, and θ: main diagonal strut angle.

The overall lateral load and deflection relationship in both specimens are finally demonstrated based on the estimated behavior of RC columns (figure 5) and the lateral load V_{cs} carried by the CB wall from equation (10) and figure 16. Figure 17 shows the calculated results where σ_m and corresponding V_{cs} are computed at the peak drift angles of 0.1, 0.2, 0.4, 0.67, 1.0, 1.5, 2.0, and 3.0%. As can be seen in the figure, the proposed procedure shows good agreement with overall lateral strength, which is the same as those under monotonic loadings (Jin 2012).

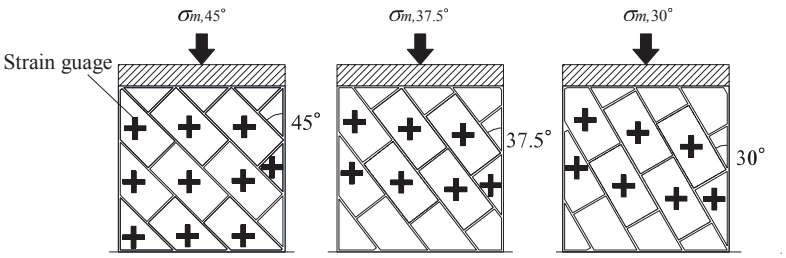

Fig. 15 Element experiments with CB prisms

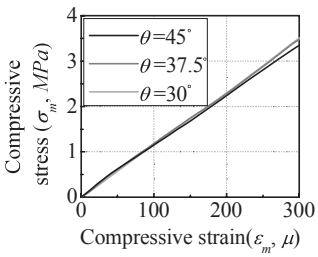

Fig. 16 σ_m-ε_m relationship

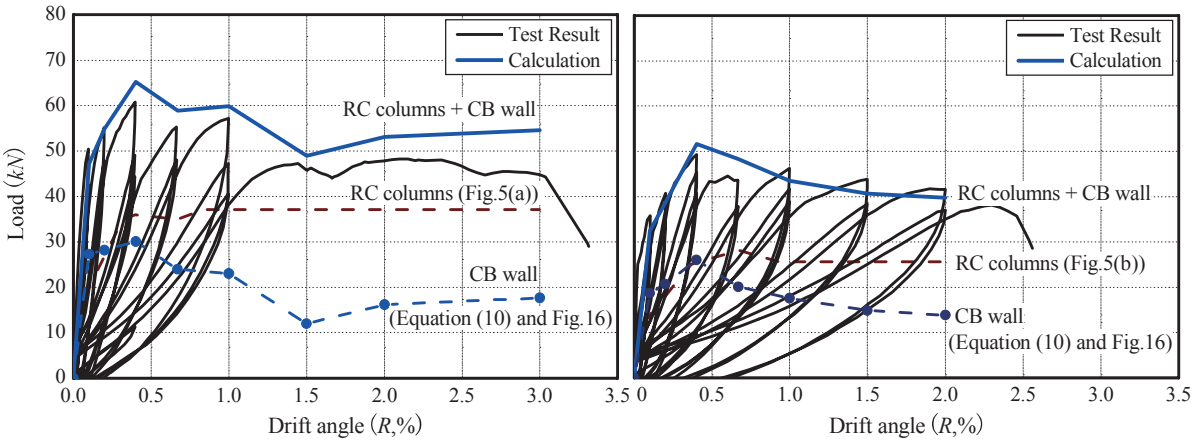

(a) IFRB specimen (b) IFFB specimen

Fig. 17 Lateral strength evaluation of both specimens

CONCLUSIONS

The seismic performance of RC frames with unreinforced CB wall for typical Korean school buildings was experimentally investigated under in-plane cyclic loadings. The major findings can be summarized as follows.

(1) The sum of shear strength of RC columns and CB wall, which is employed in the reference (FEMA 306 1998), does not show good agreement with overall lateral strength recorded in both specimens.

(2) Equivalent diagonal strut mechanism of CB wall including its main diagonal strut angle, average compressive strain, and equivalent width is evaluated using principal compressive strains on CB wall during the tests.

(3) Shear load carried by CB wall is estimated based on the compressive stress acting on the equivalent diagonal strut width calculated from the element experiments of CB prisms. The evaluation results of shear strength by the sum of both RC columns and CB wall well agree with the overall lateral strength recorded in both specimens.

(4) The shear strength of CB wall in IFRB and IFFB specimens under cyclic loadings are found slightly lower than those under monotonic loadings (Jin 2012) due to smaller principal compressive strains on diagonal strut.

ACKNOWLEDGMENT

The financial support of the JSPS Grant-in-Aid for Scientific Research (Category (B), Grant No. 21360262, Principal Investigator: Yoshiaki Nakano) and the partial support by the JSPS Grant-in-Aid for Scientific Research (Grant No. 22・9472, Investigator: Kiwoong Jin) are gratefully appreciated.

REFERENCES

Jin, K., Choi, H., Takahashi, N., Nakano, Y. (2012). “Failure mechanism and seismic capacity of RC frames with URM wall considering its diagonal strut.” Proceedings of 15th World Conference on Earthquake Engineering.

The Ministry of Construction and Transportation. (2002). “A study on the seismic evaluation and retrofit of low-rise RC Buildings in Korea (in Korean)”.

FEMA 306. (1998). “Evaluation of earthquake damaged concrete and masonry wall buildings.” Applied Technology Council (ATC-43 Project).

Architectural Instite of Japan (AIJ). (2010). “AIJ standard for structural calcuation of reinforced concerete structures.”

Architectural Instite of Japan (AIJ). (1988). “AIJ standard for structural calcuation of reinforced concerete structures.”

(Abstract Submitted: August 28, 2012)

(Accepted: September 13, 2012)